

Crack behavior of Surface Strengthened Zirconia-Alumina Composite During Indentation

A. Balakrishnan, M. C. Chu*, B. B. Panigrahi*, Je Woo Choi,
Taik Nam Kim, J. K. Park** and S. J. Cho*†

Department of Materials Engineering, Paichai University, Doma-2-Dong, Seo-Gu 439-6, Daejeon 302-735, Korea

*Division of Advance Technology, Korea Research Institute of Standards and Science,
1 Doryong-Dong, Yuseong-Gu, Daejeon 305-340, Korea

**Department of Materials Science and Engineering, KAIST, Daejeon 305-701, Korea

(2006년 11월 20일 받음, 2006년 12월 8일 최종수정본 받음)

Abstract ZTA tubes were prepared by centrifugal casting and sintered at 1600°C for 2 hrs. The ZTA tubes were machined into specimens of 3×4×40 mm. Molten Soda lime glass (SLG) was penetrated into the surface of ZTA at an optimized condition of 1500°C for the holding time of 5 h and furnace cooled. The extra glass on the surface was removed using a resin bonded diamond wheel. The glass penetrated samples were tested for their flexural strength using four point bend test. Vickers Indentation cracks were made on the glass penetrated surface at different loads of 9.8 N, 49 N, 98 N and 196 N. The residual compression on the surface enhanced the flexural strength and crack arrest behaviour remarkably. This was attributed to the thermo-elastic mismatch between the glass and ZTA matrix during cooling.

Key words residual compression, glass penetration, thermo-elastic mismatch, soda lime glass, ZTA.

1. Introduction

Various techniques have been reported to strengthen ceramics like alumina and zirconia by introducing residual compression.¹⁻³⁾ Thermal contraction mismatch between the surface region and interior induces surface residual compression during cooling. For examples, Kirchner *et al.*⁴⁾ incorporated Al₂O₃-Cr₂O₃ solid solution by heat-treating alumina in Cr₂O₃ packing powder, and Noda *et al.*⁵⁾ incorporated mullite by heat-treating alumina in contact with silicon. Though previous techniques to introduce surface compression in alumina were shown to be successful in strengthening,^{4,5)} they have a drawback in the practical standpoint. In order to strengthen ceramics, the compression should be introduced over the depth of strength-controlling surface flaws.⁶⁾ However, the techniques of Kirchner *et al.*⁴⁾ and Noda *et al.*⁵⁾ for examples, as they involve diffusion processes, require long heat-treatment times to obtain deep compression zone as compared to the depth of strength-controlling flaws (typically on the order of 50 to 200 μm). Long heat treatment would coarsen the microstructure of the ceramics, which would lead to the deterioration of properties. Previous works have shown that molten glasses penetrate into dense alumina along grain

boundaries.⁷⁻¹⁰⁾ Inspired by these previous works, we penetrate SLG glass into dense ZTA over a depth of several hundred micrometers. We confirm the existence of surface residual compression, and demonstrate the resultant strengthening.

2. Experimental

ZTA was prepared by mixing fine powders of zirconia-3 mol% yttria stabilised (NL-3YZ, NamoLab, Korea) and alumina (doped with 0.1 weight% MgO, AES-11, Sumitomo Chemicals, Japan) in the ratio (weight) of 1:9. This powder was centrifugally cast into tubes and sintered at 1600°C for 2 hours (theoretical density of ~99.8%). The flexural test specimens of 3×4×40 mm were prepared as per ISO (14704) specifications. The coefficient of thermal expansion (CTE) of ZTA was measured to be 8.4×10⁻⁶/°C using dilatometer in temperature range of 20 to 1200°C. A commercially available (Superior, Marienfeld, Germany) SLG, with the CTE of 9×10⁻⁶/°C (0-600°C) was ground into fine powder (~150 mesh), which was then spread in a thin layer on the upper surface of ZTA bar (in the area of 4×40 mm). The samples were then heated to an optimized condition of 1500°C for 5 h¹¹⁾ and allowed to cool to room temperature in the furnace itself. Micro-structural studies of the specimens were carried out with a field emission scanning electron

†E-Mail : sjcho@kriss.re.kr

microscopy (FESEM). Compositional analysis of the extra glass on the ZTA surface after thermal cycling was done by energy dispersive x-ray (EDX) analysis. The excess glass on the surface was removed by grinding carefully. Flexural strength was determined such that glass-penetrated surface was in tension during the test. Further, the penetrated glass was removed by etching by concentrated hydrofluoric (HF) acid to determine the glass penetration depth. Indentation was carried on the surface of as received and glass penetrated ZTA using Vickers Indenter was carried out under different loadings to study the crack propagation behavior.

3. Results and Discussion

Fig. 1a shows the FESEM micrograph of the cross-section of sintered ZTA (thermally etched at 1500°C for 30 min). Few very fine pores were observed at triple grain junctions. Clusters of fine zirconia particles were distributed uniformly and located at triple grain junctions of the alumina grains. Fig. 1b shows the FESEM image of the cross-section of a glass penetrated specimen. Glass was found to be diffused through the grain boundaries. The molten glass filled the residual pores and flaws which were the regions for stress concentration and hence the sources of weakness in sintered ZTA.

The extra glass on the surface was found to contain additional elements of Al and Zr during EDX analysis, indicating the dissolution of alumina and zirconia in SLG at higher temperature (Fig. 2). The EDX analysis was carried out at sufficient distance from the ZTA-glass interface in order to prevent any detection of alumina and zirconia from the ZTA matrix. The composition of the surface glass was

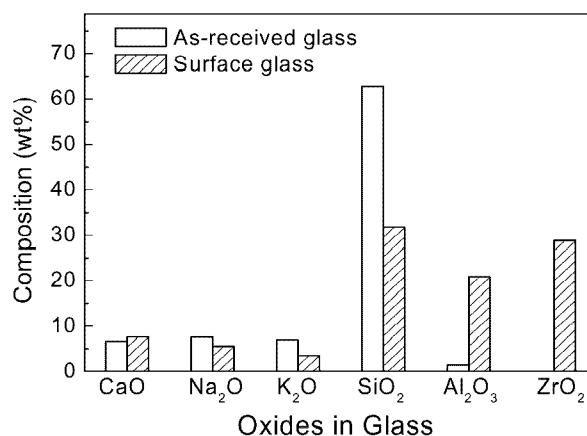


Fig. 2. EDAX analysis of the pristine glass showing significant compositional change compare to as received ZTA.

found to be same as the composition of the penetrated glass possibly due to the saturation of zirconia and alumina content of the glass. The CTE of the surface glass was predicted through the Appen's method,¹²⁾ was found to be $5.5 \times 10^{-6}/^{\circ}\text{C}$, this was relatively smaller than the CTE of SLG and ZTA.

No other crystalline phases were detected during XRD analysis except alumina and zirconia, however, the peaks were found to be shifted towards smaller diffraction angle (i.e. increase in interplaner spacing) after glass penetration (Fig. 3). The present system is a complex system where a glass-ZTA composite layer could be assumed to be coated on the ZTA substrate. Firstly, the effective CTE and elastic modulus of the glass-ZTA composite were estimated¹⁾ for different volume fraction of the glass. Then, the efforts were made to approximate the residual stress generated near interface due to the thermal expansion mismatch and elastic modulus mismatch based on available models for thin layer

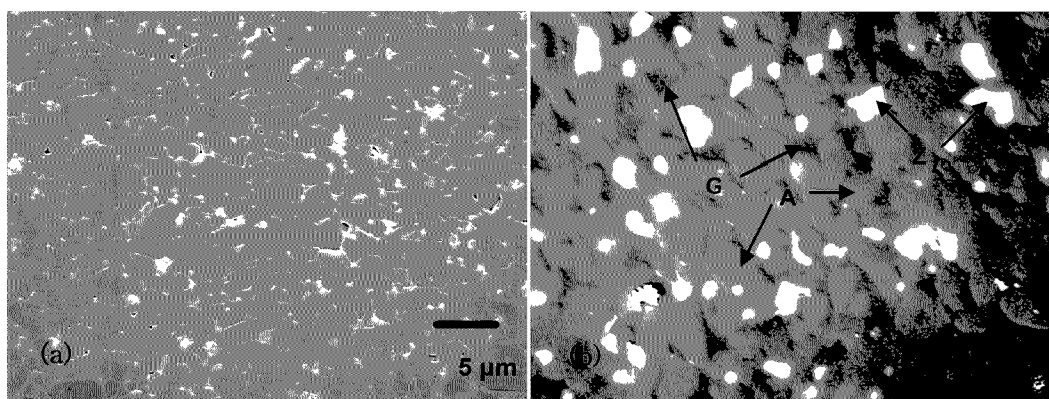


Fig. 1. a) SEM micrograph of cross-section of as received ZTA specimen (thermally etched at 1500°C for 30 min). b) SEM micrograph of cross-section of 5 hour glass penetrated ZTA, where A, G and Z indicate the alumina, glass and zirconia phase respectively.

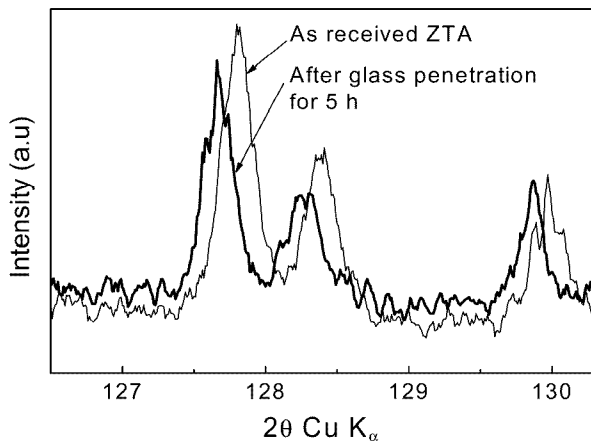


Fig. 3. XRD profile indicating high angle peak shifts for glass penetrated ZTA, showing evidence of residual compression on the surface.

coating on a substrate.^{14,15} The residual stress on the surface ZTA (glass penetrated region) was found to be about 280 MPa (compressive stress) for a glass penetration depth of 550 μm . The flexural strength (an average of 10 readings) was found to increase with increasing glass penetration to about 45% (~ 200 MPa) after 5 h (650 ± 30 MPa) compared to as-received ZTA (452 ± 50 MPa). There was a noticeable decrease crack length (of the surface region) under different loadings in the glass penetrated specimens determined by using Vickers Hardness indentation after glass penetration (Fig. 4).

The measured residual stresses (280 MPa) through XRD peak shifts¹³ are the presentation of the characteristics of the thin upper surface layer (in the glass penetrated surface), and hence yields relatively larger value compared to the increment

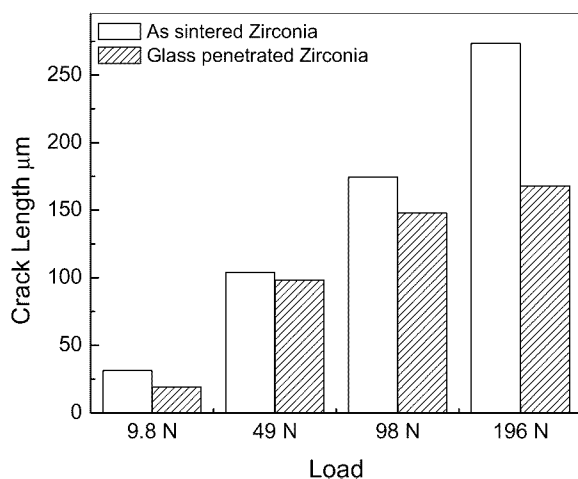


Fig. 4. Crack length during Vickers indentation test (average of five tests for each load).

observed in the strength through the flexural test (which was carried out in a bulk sample). The strengthening behavior was reported¹⁶ to depend on the crack propagation behavior and the behavior of the crack propagation depends on the nature of residual stresses. The tensile stress at the grain boundary drives the crack path along the inter-granular glass phase, whereas compressive stress follows trans-granular path and yields high bending strength. In addition, the smoothing of grains (Fig. 1b) also reduces the possible zones of stress concentration thus requiring more work for fracture. The reorientation of the crack plane causes dispersion of its energy which corresponds to a decrease in crack propagation of the material¹⁷ as seen in glass penetrated ZTA. It appears that in the present case, possibly cracks propagated through the trans-granular path. However, a clear microstructure could not be observed without etching (which may distort the microstructure), would have been helpful for more understanding. But there is no doubt that surface compressive stress does suppress crack propagation. The removal of pores in the surface region by glass-penetration may also be beneficial in obtaining the very smooth surface of ceramic products.

4. Conclusions

A significant improve in the strength of ZTA by glass incorporation at the surface was achieved in this work. Crack length decreased significantly in the glass treated specimen compared to as sintered ZTA, which was mainly attribute to the penetration surface residual compression due to thermo-elastic mismatch between the glass and ZTA.

References

1. W. D. Kingery, H. K. Bowen and D. L. Uhlmann, Introduction to Ceramics. Ch. 16, Second edition. John Wiley & Sons, New York (1976).
2. R. Tandon R, D. J. Green and R. Cook, J. Am. Ceram. Soc., **73**, 2619 (1990).
3. D. J. Green, R. Tandon and S. M. Sglavo, Science, **283**, 1295 (1999).
4. H. P. Kirchner, R. M. Gruver and R. E. Walker, J. Am. Ceram. Soc., **51**, 251 (1968).
5. S. Noda, H. Doi, T. Hioki, J.-I. Kawamoto and O. Kamigaito, J. Am. Ceram. Soc., **69**, c-210 (1986).
6. A. V. Virkar, H. W. Huang and R. A. Cutler, J. Am. Ceram. Soc., **70**, 164 (1987).
7. D. J. Green, J. Am. Ceram. Soc., **66**, c-178 (1983).
8. M. C. Chu, S. J. Cho, K. J. Yoon and H. M. Park, J. Am. Ceram. Soc., **88**, 491 (2005).
9. P. L. Flaitz and J. A. Pask, J. Am. Ceram. Soc., **70**, 449 (1987).

10. J. Jitcharoen and N. P. Padture, *J. Am. Ceram. Soc.*, **81**, 2301 (1998).
11. A. Balakrishnan, M. C. Chu, B. B. Panigrahi, K. J. Yoon, J. C. Kim, B. C. Lee, T. N. Kim and S. J. Cho, *Sol. Stat. Phenom.*, **124-126**, 1161 (2006).
12. M. B. Volf, *Mathematical Approach to Glass* (Elsevier Science Publishers, USA 1988).
13. B. D. Cullity, *Elements of X-ray Diffraction* (Addison-Wesley Publishing Co., Inc., Reading, Massachusetts, USA 1978).
14. A. Paranjpye, G. E. Beltz and N.C. MacDonald, *Modelling Simulation Mater. Sci. Eng.*, **13**, 329 (2005).
15. J. Luo and R. Stevens, *J. Eur. Ceram. Soc.*, **17**, 1565 (1997).
16. Y. Q. Wu, Y. F. Zhang, G. Pezzotti and J. K. Guo, *J. Eur. Ceram. Soc.*, **22**, 159 (2002).
17. Guazzato, M., Albakry, M., Ringer and S. P., Swain, M. V. *Dent. Mater.*, **20(5)**, 441 (2004).